Synthesis and characterization of designed peptides as inhibitors of IAPP fibrillogenesis

João Morais 79028

Integrated Master in Biological Engineering (MEBiol), Instituto Superior Técnico, University of Lisbon

Outubro de 2018

Abstract:

Type 2 diabetes (T2D) and Alzheimer's disease (AD) are characterized by the accumulation of amyloid fibrils constituted mainly by islet amyloid polypeptide (IAPP; T2D) and amyloid β peptide (Aβ, T2D). This work aimed at the optimization of solubility by maintaining the inhibitory properties of a peptide, named "peptide A", recently developed in the Kapurniotu lab.

The optimization of the solubility was done through the addition of dipeptide tags to peptide A. Analogs with tag 1 and 2, called "peptide 1" and "2", were synthesized and studied. The addition of the tags did not alter secondary structure. However, solubility was decreased and ThT binding showed that only peptide 2 can inhibit IAPP fibrillogenesis.

The study on the optimization of the inhibitory properties of peptide A was done by mutations in position X. Peptides "3" and "4" with aromatic or charged residues in position X were synthesized. The mutations with residues with different properties allowed the change of the secondary structure. The solubility studies showed, however, contradictory results. Also, peptides 3 and 4 interacted with IAPP, but only peptide 4 could inhibit the IAPP fibrillogenesis at the same molar ratio as peptide A.

In conclusion, the length of the peptide played an important role in both solubility and inhibitory properties. The shorter peptide showed a higher solubility, whereas the longer peptides showed a higher inhibitory property. In addition, inhibitory properties were affected by the nature of the amino acid residue at position X.

Introduction:

The unappropriated folding of proteins is thought to be the cause of several diseases, namely, Alzheimer's disease (AD) and Type two diabetes (T2D), among others[1–3]. The alterations in the life style of the worldwide population, as well as, the increase in the longevity were the main factors for the accentuated increase of T2D in the worldwide population[4]. Thereby, it became urgent to develop new treatments able to, at least, improve the patient's lifetime. The Alzheimer's disease is caused by the accumulation of extracellular amyloid fibrils which are composed manly by the amyloid peptide (Aβ)[5]. Aβ are natural peptides formed as a result of cellular metabolism, whose length vary at the C-terminus, between 36 to 43 amino acids[6].

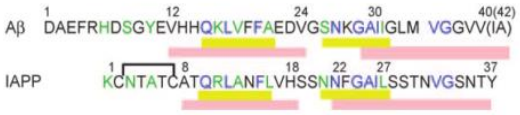

Figure 1 - Sequence of IAPP and Aβ with the identical amino acids in blue and the similar residues in green. The region highlighted in yellow are the shortest regions with a higher degree of similarity and identity. The pink area is the one reported to be important in the interaction of both peptides. Figure was taken from *A. Kapurniotu et al. (2010)*[9].

The T2D disease is characterized by the presence of amyloid fibrils produced in pancreas, designated by islet amyloid polypeptide (IAPP)[1,3]. The toxicity mechanism involved in this disease is not well understood. However, it has been proposed to interfere with cellular processes through the alteration of signaling pathways and/or cellular mechanism[7].

Several epidemiological studies have shown that patients with T2D have a higher probability to develop AD and vice-versa[8]. This predisposition can be explained by the physiological and structural similarities between both diseases[7]. The Aβ and the IAPP shared an identity and a sequence similarity of 25 % and 50%, respectively. The high degree of similarity was shared between the Aβ(15-21) and IAPP(10-16) and the Aβ(26-32) and IAPP(21-27), highlighted in yellow in figure 1[9]. The region highlighted by the pink area is the area thought to be important in the self-assembly and it contemplated the amyloidogenic region[10–15]. Interestingly, amyloid proteins can influence the appearance and progression of different amyloid diseases, through a process designated by cross-interaction or cross-seeding[16]. *In vitro* studies corroborated the existence of this process since the addition of IAPP aggregates increase the Aβ aggregation[9,17,18]. It has been reported that IAPP aggregates within the Aβ plaques in the brain of patients with both diseases, suggesting an *in vivo* correlation between both peptides[19]. Moreover, the Aβ peptides have been found in pancreatic islet amyloid aggregates of T2D[19]. A recent study *in vivo* showed the over-production of hIAPP increase the accumulation of Aβ in the brain and staining of those fibrils showed the presence of IAPP[19]. The phenome has led to the purchase of inhibitors to bind against the amyloid monomers in order to prevent their oligomerization. Previous studies have demonstrated that IAPP based peptides were capable of suppress the amyloidogenicity of IAPP and Aβ and Aβ, respectively[20]. This work aimed the biophysical characterization – conformational, binding and amyloidogenic propensities studies – of designed peptides against IAPP fibrillogenesis. More specifically, the goal was to optimize the solubility of the peptide designated as the peptide A. The increase of solubility was performed by the addition of a tag to the N-terminal region of the peptide, whereas the increase of the inhibitory properties was performed through mutations in the peptide A structure.

Material and Methods:

Peptide synthesis:

The peptides were synthesized using Fmoc solid phase peptide synthesizes (SPPS) strategy on Rink resin[21,22].

The fluorescence labelled peptide was synthesized using 3-fold molar excess of 5-(6)-carboxyfluorescein and 2-(7-aza-1H-benzotriazole-1-yl)-1,1,3,3 tetramethyluronium hexafluorophosphate (HATU) and 4,5 fold excess of N,N-diisopropylethylamine (DIEA) DIEA.

The cleavage of the peptides was done using a mixture of TFA/H2O (95%/5%) (v/v) for 3 h.

Purification of the peptides:

The peptides were purified by reverse-phase high-performance liquid chromatography (HPLC). The pre-column used was a Reprosil Gold 200 (C18 10 µm 40 x3 mm) and a Reprosil Gold 200 (C18, 10 µm 250 x8 mm) column. The elution was performed using the solution A (0,058% TFA in ddH_2O) and solution B (90% acetonitrile and 0,05% TFA in ddH_20) with different gradients. The gradient used to purify the peptides 1 and 3 started with 70% of solution A and 30% of solution B and ended with 30% of solution A and had a duration of 35 min. The peptide 2 was purified with an elution gradient, which started with 70% of solution A and 30% of solution B and ended with 30% of solution A and 70% of solution B and had a duration of 42 min. The elution gradient used to purify the peptide 4 started with 90% of solution A and 10% of solution B and ended with 10% of solution A and 90% of solution B for 30 min.

MALDI-TOF:

The confirmation of the peptide's purity was performed by MALDI-TOF MS in acetone matrix. A small amount of peptide was dissolved in acetone buffer (97% acetone, 0,1% TFA in ddH_2O).

Thioflavin-T kinetics assay:

The IAPP aliquot was dissolved in cold HFiP to have a final concentration of 1 µg/µL. After filtering the stock solution, the concentration was determined by ultraviolet (UV) at 274 nm. The peptides aliquots were dissolved in cold HFiP to have a final concentration of 1 mM.

The incubation of IAPP was performed with an IAPP concentration of 16,5 µM. The peptides were tested in different ratios: 1:1, 1:2, 1:5 and 1:10. Firstly, the correct amount of volume from IAPP stock was pipetted to an Eppendorf tube. In the Eppendorf tubes with a mixture, the peptide was pipetted into the IAPP solution. Afterwards, the HFiP was evaporated using air and then added the ThT buffer (50 mM Na_2PHO_4, 100 mM NaCl in ddH_2O, pH=7,4), containing 0,5% of HFiP. Afterwards, the samples were vortexed and 30 µL of solution was transferred to a 96 well microtiter plate. With a multi-channel pipette, 170 µL of 20 µM ThT solution was transferred to the microtiter plate and mixed. The measurements were performed from 24 to 24h during a week and the incubations were kept at 20 ^oC. Finally, the fluorescence was measured in the 2030 Multilabel Reader VictorX3 (PerkinElmer Life Sciences).

TEM:

10 µL of aliquots of solution used for the ThT assay was applied for 3 min on carbon-coated grids after the 7 days of incubation. Afterwards the solution was removed and the grid and washed with 10 µL of distilled water. Lastly, 10 µL of % (w/v) uranyl acetate was applied for 1 min to stain. The examination of the grids was performed with a JEOL JEM 100CX electron microscope at 100 kV.

Circular dichroism:

Far-UV CD measurements were carried out using a Jasco 715 spectropolarimeter. Spectra were collected between 195 and 250 nm at 0.1 nm intervals, a response time of 1 second.

Concentration dependence: The peptide stock solution was prepared through the addition of cold HFiP to have a final concentration of 1 mM. The peptides concentration tested were 5 µM, 10 µM, 20 µM, 50 µM, 100 µM. The first concentration was tested in the 1 cm cuvette length, the last concentration in the 0,2 cm cuvette and the rest were tested with the 0,5 cm cuvette. The measurements were performed in 1xb (10 mM Na_2PHO_4 in ddH_2O, physiological pH) containing 1% of HFiP. When the peptide started to aggregate, the measurements were stopped.

Interaction with IAPP

The stock of IAPP and a 1 mM peptide stock in HFiP were prepared. This assay was performed with 1 cm cuvette in in 1xb (10 mM Na_2PHO_4 in ddH_2O, physiological pH) containing 1% of HFiP. The IAPP alone (5 µM), the peptide alone (10 µM) and the mixture of IAPP and peptide (1:2) was measure for the following time points: 0h,5 min, 15 min, 30 min, 1h, 7h, 24h.

Fluorescence spectroscopy:

Fluorescence measurements were performed with a JASCO FP-6500 fluorescence spectrophotometer. The fluorescence spectroscopy titrations were used to determine the dissociation constant of the binding of fluorescence labelled peptide to IAPP and peptide and the binding of fluorescence labelled IAPP to peptide.

To prepare the fluorescence labelled peptide stock remove with a pipette tip a small amount and dissolved it in 200 µL of HFiP. After the peptide was completely dissolved, it was filtered with a Millipore filter, previously soaked in HFiP, and the concentration was determined by UV at 432 nm. Afterwards, the concentration of the stock had to be adjusted to 1 µM. The stock solution of the unlabeled peptide was prepared with a concentration of 1 mM. Afterwards, several dilutions were prepared in order to have a final concentration in the Eppendorf tube of 500, 250, 100, 50, 25, 10, 5 ,2,5 and 1 µM. The dilutions were prepared in triplicate. In the cases, where the plateau is not reached higher or lower concentrations had to be prepared. The measurements were performed from 500 nm to 600 nm, in 1xb (10 mM Na_2PHO_4 in ddH_2O, physiological pH) buffer with 1% of HFiP using a 10.000 mm cuvette with a final volume of 500 µL.

Centrifugation assay:

The centrifugation of the peptide 3 and 4 were performed at 20 µM. Three different time point were measured: 0h, 20 min and 7

days. The preparation of the samples was the same. To have 1 µg of peptide in each eppi, the correct volume was transferred from 100 µM of peptide stock solution previously dissolved in HFiP. The HFiP was let to evaporate alone and then 1xb (10 mM Na_2PHO_4 in ddH_2O, physiological pH) was added in order to have a final concentration of 20 µM. Each incubation was prepared in triplicated. The 7 days incubation were incubated over the bench at room temperature. Afterwards, the 20 min and the 7 days incubations were centrifuge at 19900xg for 20 min. The supernatant was transferred to new Eppendorf tubes (this step was done to all the incubations) and the 1xb was added to have a final volume of 50 µL. The pellet samples were resuspended in 50 µL. The BCA solution was prepared in the ratio 25:24:1 for A:B:C, respectively. After the preparation and mixing of the BCA solution, 150 µL was transferred to all Eppendorf tubes and mixed. The Eppendorf tubes were incubated for 3h at 37 ^{o}C. Then, the Eppendorf tubes were put at -20 ^{o}C for 5 min. Lastly, the solutions were transferred to a 96-well sterile plate and the fluorescence was measured at 570 nm.

Results and discussion:

The structure-activity relationship of the peptides was performed to optimize the solubility and the inhibition of the IAPP fibrillogenesis. The solubility optimization was performed by the addition of tags to the N-terminus of the peptide A. On the other hand, the optimization of inhibitory properties was performed by mutations in position X within the core structure of the peptide A.

Initially the secondary structure as well as the solubility of the peptides were analyzed by CD. The results showed in figure 2 that the peptide A had a β-sheet/β-turn secondary structure. The addition of tag 1 and 2 did not change the secondary structure of the peptides 1 and 2 in comparison with the peptide A. However, these modifications decreased the solubility of the peptide 1 and 2 in comparison with the peptide A. The peptides 1 and precipitated at 20 and 50 µM, while the peptide A precipitated at 100 µM. The significant decrease of the solubility of the peptide 1 could be due to non-covalent interactions between the N and the C-terminus residues of the peptide. The results obtained for the peptide 2 corroborated that hypothesis since the two tags only differed in N-terminus amino acid and the solubility of the peptide improved in comparison to the peptide 1.

The results obtained for the peptides 3 and 4 showed different results. The exchange of the residue in position X by an aromatic residue did not change the secondary structure. However, the introduction of a charged residue in position X allowed the appearance of random coil structure. This modification was particularly interesting since the random coil content is important for the increase of solubility. The solubility of the peptide 3 and 4 were 50 and 100 µM, respectively. The introduction of the aromatic residue in position X managed to establish non-covalent interactions which stabilize the β-sheet/ β-sheet structure. The introduction of a hydrophobic amino acid in the core structure of the inhibitor decreased due to the increase of the peptide hydrophobicity. On the other hand, the

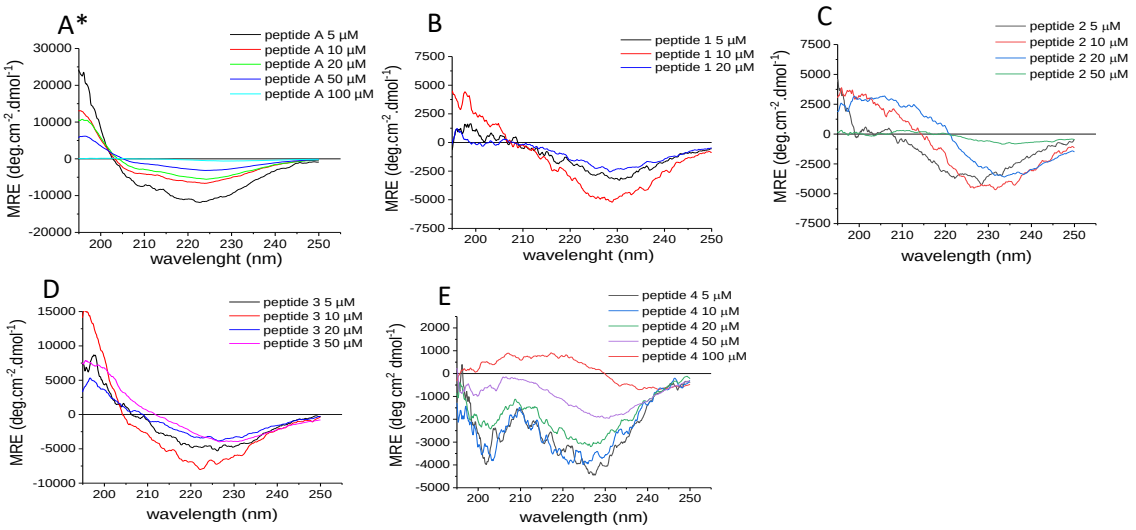

Figure 2 - Far UV CD – concentration dependence spectra obtained for all the peptides. The peptides were dissolved in 1xb containing 0,5 % HFiP, at room temperature. The determination of the peptide solubility was performed at 5, 10, 20, 50 and 100 µM. The concentrations were tested until visible precipitation was observed in the cuvette. The 5 µM measurement was performed in a 1 cm cuvette, whereas the 10, 20 and 50 µM were performed at a 0,5 cm cuvette. Lastly, the 100 µM concentration was done in a 0,2 cm cuvette. A – peptide A. B – peptide 1. C – peptide 2. D – peptide 3. E – peptide 4.

**Armiento, Kapurniotu et al.* unpublished

introduction of a charged residue enabled the destabilization of the core structure which explained the appearance of the random coil structure.

To further analyze the solubility of the peptides 3 and 4 a centrifugation assay was performed. The results in figure 3 showed that the peptide 3 (figure 3 A) and the peptide 4 (figure 3 B) precipitated at 20 µM. This result was inconsistent with the CD-concentration dependence results. A possible explanation for the differences could be non-specific binding of the peptide to the plastic walls of the Eppendorf tube. To

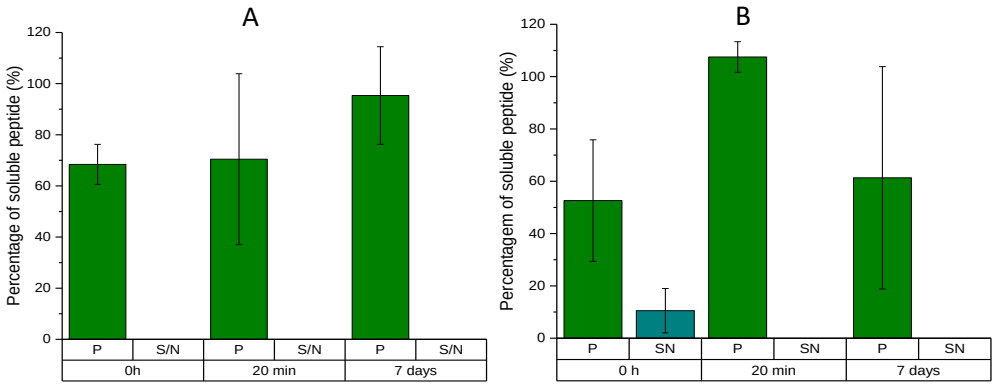

Figure 3 - Centrifugation assay with 20 µM peptide. The peptide was dissolved in 1xb at room temperature. The measurements were performed at three different time points: 0h, 20 min and 7 days. The peptide soluble in the pellet and supernatant fractions were determined by BCA assay. Data shown are the mean value from 3 assays ±SD. A – Results obtained for the peptide 3. B – Results obtained for the peptide 4.

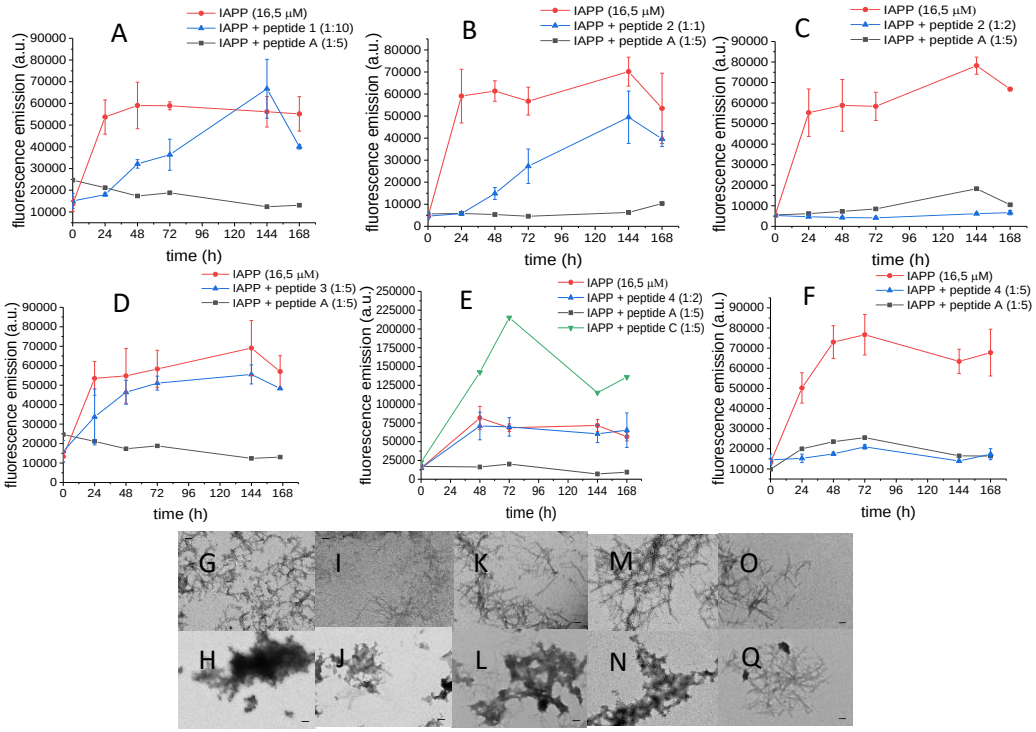

Figure 4 – ThT assay of the mixture IAPP with the peptides and TEM images. The peptides were dissolved in ThT buffer, containing 0,5 % of HFiP. The Eppendorfs were incubated at 20 ºC and experiment was followed through 7 days and the measurements were done every 24h. The IAPP kinetics was represent in red (mean ± SD, n=3), the mixture of the IAPP and the peptides were represented in blue (mean ± SD, n=3), the control was represented in grey (n=1) and the peptide C was represented in green (n=1). A- IAPP plus peptide 1 in the ratio 1:10. B- IAPP plus peptide 2 in the ratio 1:1. C- IAPP plus peptide 2 in the ratio 1:2. D- IAPP plus peptide 3 in the ratio 1:5. E- IAPP plus peptide 4 in the ratio 1:2. F- IAPP plus peptide 4 in the ratio 1:5. G-H – TEM pictures for the mixture between IAPP and the peptide 1 (1:10) taken for 7 days. G- fibrils. H- amorphous. I-J – TEM pictures for the mixture between IAPP and the peptide 2 (1:1) taken for 7 days. I- fibrils. J- amorphous. K-L – TEM pictures for the mixture between IAPP and the peptide 2 (1:2) taken for 7 days. K- fibrils. L- amorphous. M-N – TEM pictures for the mixture between IAPP and the peptide 3 (1:5) taken for 7 days. M- fibrils. N- amorphous. O-Q – TEM pictures for the mixture between IAPP and the peptide 4 (1:2) taken for 7 days. O- fibrils. Q- amorphous.

notice that the composition and configuration of the surface plays an important role in the establishment of non-covalent interactions of the peptides with the surface.

The ability of the peptides to inhibit the IAPP fibrillogenesis was tested by ThT assay and the results were confirmed by TEM. The ThT had the ability to bind to amyloid fibrils and that interaction was responsible for the fluorescence emission of the thioflavin-T[23,24]. The result of inhibition of IAPP fibrillogenesis are showed in figure 4. The peptide 1 was not able to inhibit the IAPP fibrils formation for the ratio 1:10, as it is shown in figure 4 A. The TEM results in figure 4G-H showed 90% of fibrils and 10% of amorphous. The figures 4 B-C showed the results for the peptide 2. At a ratio of 1:2 the fluorescence remained low, suggesting that the peptide inhibit the

IAPP fibrillogenesis. For the ratio 1:1 the peptide was no longer able to inhibit the IAPP fibrils formation and the fluorescence emission increased after 24h. Hence, the inhibitory properties of the peptide increased in comparison with the peptide A. As a control, the peptide A was used in a ratio 1:5, in which it inhibited the IAPP fibril formation *(Armiento, Kapurniotu et al.* unpublished). However, the TEM results in figure 4 I-L showed the presence of fibrils at both ratios what was inconsistent with the ThT results. The ThT results suggested that the amino acid in the N-terminus of the peptide played an important role in the inhibitory properties of the peptide. However, charged residues could destroy the inhibitory properties possibly due to the establishment of non-covalent interactions with the C-terminal residue.

The mutations in position X of the structure of peptide A led to different results. The introduction of an aromatic residue strongly affected the inhibitory properties of the peptide as it is showed in figure 4D. Since the peptide alone was precipitating at a concentration of 82,5 μM, the other ratios were not tested. The TEM result in figure 4M-N showed the presence of fibrils for the ratio 1:5, which corroborated the ThT results. On the other hand, the introduction of a charged residue in position X led to the destabilization of the hydrophobic core of the peptide. This modification enabled the peptide to inhibit IAPP fibrillogenesis at a ratio 1:5, but not at a ratio 1:2, as it is showed in figure 4 E-F. Thus, this alteration did not change the peptide inhibition properties. The TEM results for the ratio 1:2 showed the presence of 30% of fibrils and 70% of amorphous. The percentage of fibrils obtained was lower than the expected and new TEM grids should be prepared.

Afterwards, the interaction of the designed peptides was confirmed by CD and fluorescence spectroscopy titration.

The first experiment measured weather the secondary structure of the mixture IAPP and peptide changed over time due to the interaction of both peptides. The results are showed in figure 5. In this experiment three measurements were made in parallel: the IAPP and the peptide alone and the mixture of IAPP and the peptide. For the several experiments the IAPP structure switch from random coil to β-sheet and the structures of the peptides did not change over time. The structures of the mixture of the peptide 1 and 2 change over time since the shape of the mixture curve at 24h was different from the theoretical sum of IAPP and peptide alone structures. This comparison was important since the CD results give an average conformation. In the case, where the shape of the curves was similar, then we could not conclude anything regarding the binding of IAPP to the peptide. Thus, these results showed that IAPP and the peptides 1 and 2 interact with IAPP and due to that interaction, the secondary structure changed. Moreover, the addition of the tags did not alter the interaction of the peptide with IAPP.

The shape of the curves of the mixture between IAPP and the peptide 3 and 4 were also different from the theoretical sum. In the case of peptide 4 a detailed view (plot of the two local minima) showed the increase of the random coil content.

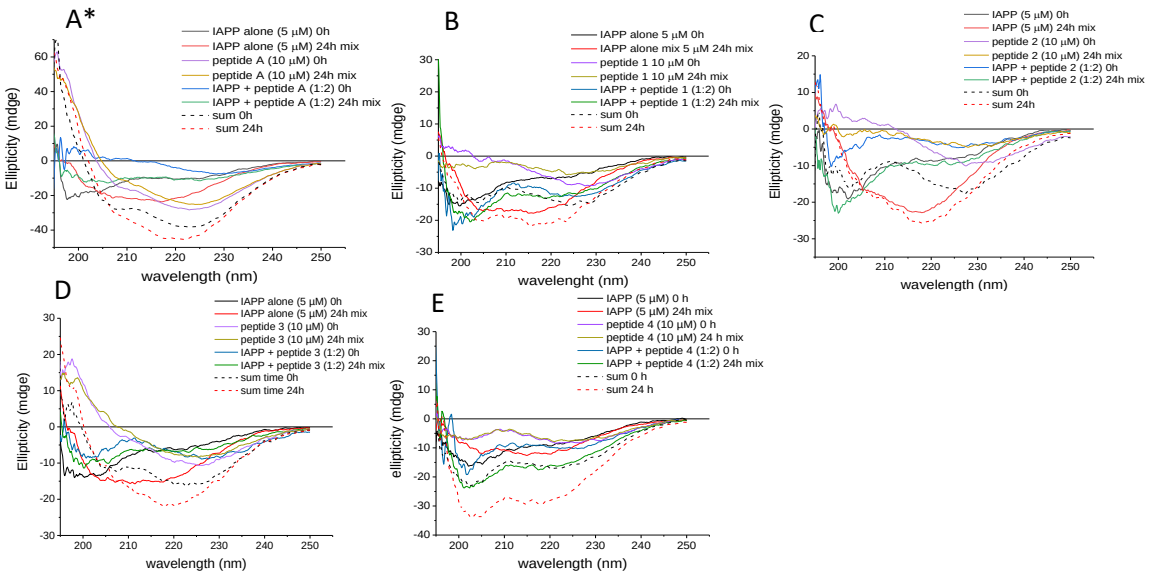

Figure 4 - Far UV CD spectra obtained for the interaction of IAPP and the peptides. The peptides were dissolved in 1xb containing 0,5% HFiP, at room temperature. Three different measurements were measured in parallel: the IAPP alone (5 μM), the peptide alone (10 μM) and the mixture of both peptides (1:2). The measurements were done in 1 cm cuvettes. The interaction of the peptides was tested over time, more specifically, 0h, 5 min, 15 min, 30 min, 1h, 7h and 24h. A- Interaction between IAPP and the peptide A. B – Interaction of IAPP and peptide 1. C – Interaction of IAPP and peptide 2. D – Interaction of IAPP and peptide 3. E – Interaction of IAPP and peptide 4.

**Armiento, Kapurniotu et al.* unpublished

The peptide 3 and the peptide 4 also interacted with IAPP which meant the mutations in the position X did not change the ability of the peptide to interact with IAPP. Furthermore, the nature of the residue in position X seemed not to be important for the interaction with IAPP.

The fluorescence spectroscopy titration experiments were performed to determine the apparent dissociation constant between IAPP and the fluorescence labelled peptide, peptide and the fluorescence labelled IAPP and the self-assembly of the peptide (interaction between fluorescence labelled peptide and the peptide). The first two constants enabled to understand weather the peptide bound to oligomeric or monomeric IAPP. The results are showed in table 1. The results showed that the peptide A was only able to bind to monomeric IAPP. Thus, inhibition of IAPP fibrillogenesis depended only in the binding of the peptide to IAPP monomers. The addition of the tags 1 and 2 to the N-terminus of the peptide did not alter the self-assembly dissociation constants neither the dissociation constant of the binding to monomeric IAPP. However, the addition of this tags allowed the binding to oligomeric IAPP. The inhibition assay showed that the only the peptide 2 enabled the inhibition of IAPP fibrillogenesis. Thus, there is no relationship between the inhibition properties of the peptide and the binding of the peptide to IAPP. The mutations in position X of the peptide A

Table 1 – Apparent K_D mean values ± SD obtained for three different experiments: the determination of the binding affinity between the fluorescence labelled peptide and IAPP; the binding affinity between the fluorescence IAPP and the peptide and the binding activity between the fluorescence labelled peptide and the peptide. The experiments were performed in triplicates and used 5 nM of the fluorescence labelled peptide with the increase concentration of the peptides in 1xb (10 mM phosphate buffer, pH=7,4) containing 1% HFiP at room temperature.

	App. K_D fluorescence labelled peptide + IAPP (nM)	App. K_D fluorescence labelled IAPP + peptide (nM)	App. K_D fluorescence labelled peptide + peptide (nM)
Peptide A	n.b.[a] *	26,3 ± 5,9*	65,9 ± 26,3*
Peptide 1	24,5 ± 3,57	66,3 ± 33,4	39,6 ± 4,3
Peptide 2	47,6 ± 5,4	103,4 ± 2,4 (24,0±4,2)	49,6 ± 8,6
Peptide 3	167 ± 18	25,7 ± 14,2	99,5 ± 19,7
Peptide 4	56,8 ± 20,3	37,6 ± 17,3	31,9 ± 10,7

* *Armiento, Kapurniotu et al.* unpublished. [a] n.b. – no binding

changed the binding properties of the peptides 3 and 4 in comparison with the peptide A. The substitution of the residue at position X by an aromatic/hydrophobic or acharged residue allowed the binding of the peptide to IAPP oligomers. Thus, the residue in position X plays an important role in the binding properties of the peptides. Nevertheless, the binding of peptide 3 was 10 times lower than the peptide 4. This result suggested that the decreased of the hydrophobicity of the peptide in that region was important for the binding to oligomeric IAPP. This mutation did not change the binding affinity of those peptides toward monomeric IAPP. Since the peptide 3 did not inhibit IAPP fibrils formation and peptide 4 did, there was no correlation between the dissociation constants and the inhibition properties of the peptides.

Conclusion:

In conclusion, the approaches used to optimize the peptides properties did not had the expected results. The addition of tags to the N-terminus of the peptide decreased the peptides solubility but increased the inhibition properties of IAPP fibrils formation. On the other hand, the specific mutations in position X of the core structure of the peptide A did not increase the solubility neither the inhibitory properties of the peptide, in comparison with peptide A. Hence, the longer peptides displayed better inhibitory properties and the shortest peptides showed a higher solubility.

Nevertheless, these modifications provided important information about the importance of some positions in the core structure of peptide A and how they affect the peptides properties. Thus, this information could be used for the development of better inhibitors against IAPP fibrillogenesis.

Bibliography:

1. Höppener, J. W., Ahrén, B. & Lips, C. J. Islet amyloid and type 2 diabetes mellitus. *N. Engl. J. Med.* **343,** 411–419 (2000).
2. Enserink, M. First Alzheimer's Diagnosis Confirmed. *Science (80-.).* **279,** 2037 LP-2037 (1998).
3. Fonseca, V. A. Defining and characterizing the progression of type 2 diabetes. *Diabetes Care* **32 Suppl 2,** (2009).

4. Shaw, J. E., Sicree, R. A. & Zimmet, P. Z. Global estimates of the prevalence of diabetes for 2010 and 2030. *Diabetes Res. Clin. Pract.* **87,** 4–14 (2010).
5. Manuscript, A. Synapses and Alzheimer ' s disease. 1–18 (2013). doi:10.1101/cshperspect.a005777.Synapses
6. Henry W. Querfurth, M.D., Ph.D., and Frank M. LaFerla, P. . Mechanisms of Alzheimer's Disease. *N. Engl. J. Med. 362,* **362,** 329–344 (2010).
7. Li, L. & Hölscher, C. Common pathological processes in Alzheimer disease and type 2 diabetes: A review. *Brain Res. Rev.* **56,** 384–402 (2007).
8. Haan, M. N. Therapy insight: Type 2 diabetes mellitus and the risk of late-onset Alzheimer's disease. *Nat. Clin. Pract. Neurol.* **2,** 159–166 (2006).
9. Andreetto, E. *et al.* Identification of hot regions of the Aβ-IAPP Interaction interface as high-affinity binding sites in both cross- and self-association. *Angew. Chemie - Int. Ed.* **49,** 3081–3085 (2010).
10. Ritter, C. *et al.* 3D structure of Alzheimer ' s amyloid- beta (1 – 42) fibrils. (2005).
11. Shim, S.-H. *et al.* Two-dimensional IR spectroscopy and isotope labeling defines the pathway of amyloid formation with residue-specific resolution. *Proc. Natl. Acad. Sci.* **106,** 6614–6619 (2009).
12. Mazor, Y., Gilead, S., Benhar, I. & Gazit, E. Identification and characterization of a novel molecular-recognition and self-assembly domain within the islet amyloid polypeptide. *J. Mol. Biol.* **322,** 1013–1024 (2002).
13. Tenidis, K. *et al.* Identification of a penta- and hexapeptide of islet amyloid polypeptide (IAPP) with amyloidogenic and cytotoxic properties. *J. Mol. Biol.* **295,** 1055–1071 (2000).
14. Petkova, A. T. *et al.* A structural model for Alzheimer's β-amyloid fibrils based on experimental constraints from solid state NMR. *Proc. Natl. Acad. Sci. U. S. A.* **99,** 16742–7 (2002).
15. Luca, S., Yau, W. M., Leapman, R. & Tycko, R. Peptide conformation and supramolecular organization in amylin fibrils: Constraints from solid-state NMR. *Biochemistry* **46,** 13505–13522 (2007).
16. Luo, J., Wärmländer, S. K. T. S., Gräslund, A. & Abrahams, J. P. Cross-interactions between the Alzheimer disease amyloid-β peptide and other amyloid proteins: A further aspect of the amyloid cascade hypothesis. *J. Biol. Chem.* **291,** 16485–16493 (2016).
17. Hammond, C. & Helenius, A. Quality control in the secretory pathway. *Isr. Med. Assoc. J.* **8,** 238–42 (2006).
18. Tartaglia, G. G. *et al.* Prediction of Aggregation-Prone Regions in Structured Proteins. *J. Mol. Biol.* **380,** 425–436 (2008).
19. Moreno-Gonzalez, I. *et al.* Molecular interaction between type 2 diabetes and Alzheimer's disease through cross-seeding of protein misfolding. *Mol. Psychiatry* **22,** 1327–1334 (2017).
20. Andreetto, E. *et al.* A Hot-Segment-Based Approach for the Design of Cross-Amyloid Interaction Surface Mimics as Inhibitors of Amyloid Self-Assembly. *Angew. Chemie - Int. Ed.* **54,** 13095–13100 (2015).
21. Yan, L.-M., Tatarek-Nossol, M., Velkova, A., Kazantzis, A. & Kapurniotu, A. Design of a mimic of nonamyloidogenic and bioactive human islet amyloid polypeptide (IAPP) as nanomolar affinity inhibitor of IAPP cytotoxic fibrillogenesis. *Proc. Natl. Acad. Sci. U. S. A.* **103,** 2046–51 (2006).
22. Bakou, M. *et al.* Key aromatic/hydrophobic amino acids controlling a cross-amyloid peptide interaction versus amyloid self-assembly. *J. Biol. Chem.* **292,** 14587–14602 (2017).
23. Biancalana, M., Makabe, K., Koide, A. & Koide, S. Molecular Mechanism of Thioflavin-T Binding to the Surface of β-Rich Peptide Self-Assemblies. *J. Mol. Biol.* **385,** 1052–1063 (2009).
24. Wu, C., Biancalana, M., Koide, S. & Shea, J. E. Binding Modes of Thioflavin-T to the Single-Layer β-Sheet of the Peptide Self-Assembly Mimics. *J. Mol. Biol.* **394,** 627–633 (2009).